



## Data Article

# Dataset on investigating nucleation and growth kinetics of methane hydrate in aqueous methanol solutions



Anton P. Semenov<sup>a,\*</sup>, Timur B. Tulegenov<sup>a</sup>, Rais I. Mendgaziev<sup>a</sup>,  
Andrey S. Stoporev<sup>a</sup>, Vladimir A. Istomin<sup>a,b</sup>, Daria V. Sergeeva<sup>a,b</sup>,  
Daniil A. Lednev<sup>a</sup>, Vladimir A. Vinokurov<sup>a</sup>

<sup>a</sup> Gubkin University, Department of Physical and Colloid Chemistry, 65 Leninsky prospekt, Building 1, Moscow 119991, Russia

<sup>b</sup> Skolkovo Institute of Science and Technology (Skoltech), 30 Bolshoy Boulevard, p. 1, Moscow, 121205, Russia

## ARTICLE INFO

**Article history:**

Received 1 April 2024

Accepted 6 May 2024

Available online 17 May 2024

Dataset link: [Raw data from the investigation of methane hydrate nucleation and growth kinetics in the methane–water and methane–methanol–water systems \(Original data\)](#)

**Keywords:**

Gas hydrates

Thermodynamic hydrate inhibitor

Kinetic hydrate promoter

Kinetic hydrate inhibitor

Gas hydrate nucleation

Gas hydrate growth

## ABSTRACT

This work systematically investigates the effect of methanol (MeOH) in a wide range of concentrations (0, 1, 2.5, 5, 10, 20, 30, 40, and 50 mass%) on methane hydrate nucleation and growth kinetics. Multiple measurements of gas hydrate onset temperatures and pressures for CH<sub>4</sub>–H<sub>2</sub>O and CH<sub>4</sub>–MeOH–H<sub>2</sub>O systems were performed by ramp cooling experiments (1 K/h) using sapphire rocking cell RCS6 apparatus. The dataset comprises 96 ramp experiments conducted under identical initial conditions for each solution (gas pressure of 8.1 MPa at 295 K). The reported hydrate onset temperatures and pressures range within 248–282 K and 6.2–7.5 MPa, respectively. The methane hydrate onset subcooling was calculated using literature data on the three-phase gas–aqueous solution–gas hydrate equilibrium for the studied systems. The study determined the numerical values of the shape and scale parameters of gamma distributions that describe the empirical dependences of methane hydrate nucleation cumulative probability as a function of hydrate onset subcooling in the aqueous methanol solutions. Gas uptake curves were analyzed to characterize the kinetics of methane

DOI of original article: [10.1016/j.molliq.2024.124780](https://doi.org/10.1016/j.molliq.2024.124780)

\* Corresponding author.

E-mail address: [semenov.a@gubkin.ru](mailto:semenov.a@gubkin.ru) (A.P. Semenov).

<https://doi.org/10.1016/j.dib.2024.110517>

2352-3409/© 2024 The Author(s). Published by Elsevier Inc. This is an open access article under the CC BY-NC-ND license (<http://creativecommons.org/licenses/by-nc-nd/4.0/>)

hydrate growth under polythermal conditions at different methanol concentrations.

© 2024 The Author(s). Published by Elsevier Inc.

This is an open access article under the CC BY-NC-ND license (<http://creativecommons.org/licenses/by-nc-nd/4.0/>)

## Specifications Table

Subject	Chemistry
Specific subject area	Physical and Theoretical Chemistry
Type of data	Tables, figures Raw, analyzed
Data collection	Ramp cooling experiments (1 K/h) were used to study the kinetics of nucleation and growth of methane hydrate in CH <sub>4</sub> -H <sub>2</sub> O and CH <sub>4</sub> -H <sub>2</sub> O-methanol (MeOH) systems. The onset of methane hydrate in two-phase systems of methane gas-aqueous solution was measured in terms of temperature, pressure, and subcooling (difference between the equilibrium temperature and the onset temperature at a given pressure) during fluid mixing by rocking the test cells of the RCS6 apparatus (PSL Systemtechnik). The dataset comprises 96 ramp cooling experiments. The experiments were conducted using nine different methanol concentrations in an aqueous solution, ranging from 0 (pure water) to 50 mass% MeOH. The initial experimental conditions were identical for all samples: a pressure of 8.1 MPa at 295 K, with a volume of 10 mL for each solution sample. The hydrate onset temperatures and pressures fell within 248–282 K and 6.2–7.5 MPa, respectively. Using experimental data on the three-phase gas-aqueous solution-gas hydrate equilibrium in the methane-methanol-water system [1,2], the hydrate onset subcooling was calculated based on the measured hydrate onset temperature and pressure values.
Data source location	Gubkin University, Department of Physical and Colloid Chemistry, Moscow, Russia. 55.692232°N, 37.55487°E
Data accessibility	Repository name: Mendeley Data Data identification number: <a href="https://data.mendeley.com/datasets/324kyf7czt/1">10.17632/324kyf7czt.1</a> Direct URL to data: <a href="https://data.mendeley.com/datasets/324kyf7czt/1">https://data.mendeley.com/datasets/324kyf7czt/1</a>
Related research article	A.P. Semenov, T.B. Tulegenov, R.I. Mendgaziev, A.S. Stoporev, V.A. Istomin, D. V. Sergeeva, D.A. Lednev, V.A. Vinokurov, Dual nature of methanol as a thermodynamic inhibitor and kinetic promoter of methane hydrate formation in a wide concentration range, J. Mol. Liq. 403 (2024) 124780. <a href="https://doi.org/10.1016/j.molliq.2024.124780">https://doi.org/10.1016/j.molliq.2024.124780</a> [3].

## 1. Value of the Data

- The data shed light on the role of methanol over a wide range of concentrations in aqueous solution in the nucleation and growth processes of methane hydrate.
- The data allows for determining the kinetic parameters of methane hydrate formation from water and aqueous methanol solutions.
- The data can be used to compare the effects of methanol and other compounds on methane hydrate nucleation kinetics under polythermal conditions.
- The data could be valuable for developing new mathematical models describing methane hydrate nucleation and growth kinetics.
- The data can serve as a reference for comparing methanol and other kinetic promoters of methane hydrate growth.

## 2. Background

Methanol (MeOH) is the major thermodynamic inhibitor of gas hydrates and is frequently used as an anti-hydrate chemical in the oil and gas industry. The thermodynamics of gas hy-

hydrate formation in aqueous methanol solutions has been extensively studied [1,2,4–9]. The impact of methanol on methane hydrate nucleation and growth kinetics has not been thoroughly examined across a broad range of MeOH concentrations relevant to its use as a thermodynamic inhibitor in industry. The literature presents results from experiments and MD simulations on the impact of low concentrations of methanol (usually ranging from tens of ppm to 10 mass%) on the kinetics of gas hydrate formation [10–18]. There is a single paper where the kinetics of methane hydrate nucleation in the presence of methanol in a wide range of concentrations (up to 50 mass%) has been studied using MD simulations [19]. However, these results have not been experimentally verified. We conducted a systematic experimental study to fill this gap. The results include the determination of kinetic parameters such as methane hydrate onset temperature, pressure, subcooling, gas uptake quantity, and gas uptake rate in  $\text{CH}_4\text{-H}_2\text{O}$  and  $\text{CH}_4\text{-H}_2\text{O-MeOH}$  systems. The new results answer the fundamental question of how different methanol concentrations affect the kinetics of methane hydrate nucleation and growth. The obtained data deepened the understanding of the role of methanol in various stages of the gas hydrate formation process.

### 3. Data Description

The data in the folder "Gas hydrate kinetics  $\text{CH}_4\text{-MeOH-H}_2\text{O}$ " (see link <https://data.mendeley.com/datasets/324kyf7czt/1>) are associated with the study of methane hydrate nucleation and growth kinetics in the methane–water and methane–methanol–water systems. Each subfolder in the directory is named after the composition of the aqueous solution under study. For instance, the subfolder labeled '1 % MeOH' contains experimental data collected during the investigation of methane hydrate nucleation and growth in the presence of an aqueous methanol solution with a feed alcohol concentration of 1 mass%. Every subfolder includes multiple .xlsx files. Each file represents the raw experimental data recorded in one of the cooling–heating cycles. For instance, the '1 % MeOH\_1 cycle' file includes experimental data obtained for a sample of 1 mass% aqueous methanol solution in the first cooling–heating cycle. Three to five cooling–heating cycles were conducted for each sample to get a statistically significant dataset for calculating methane hydrate formation probability distributions and determining methane hydrate nucleation rates. The file contains data on time (since cycle start, column A), thermostatic bath temperature (in degrees Celsius, column C), and gauge pressure in Cells #1–6 (in bars, columns K–P) of the RCS6 apparatus.

The original research paper presents an example of the experimental curves obtained for 10 mass% MeOH sample after two cooling–heating cycles. It also includes determining the onset temperature  $T_o$  and pressure  $P_o$  of methane hydrate (refer to Fig. 1 in ref. [3]). Table 1 presents all measured values of the kinetic parameters, including an additional column with the values of hydrate onset subcooling  $\Delta T_o$  (the difference between the temperature at the three-phase equilibrium line of methane–aqueous methanol solution–methane hydrate at pressure  $P_o$  according to [1,2] and  $T_o$ ). The mean  $\pm$  standard deviation of the indicated kinetic parameters are shown in bold in the gray-filled row for each sample in Table 1. The cumulative probability distributions of methane hydrate nucleation  $F$  as a function of hydrate onset subcooling were approximated by the integral gamma distribution function (Fig. 5 in ref. [3]). Table 2 provides the numerical values of the gamma distribution coefficients (shape parameter  $a$ , scale parameter  $b$ , and adjusted  $R^2$ ) for each aqueous methanol solution.

Figs. 1–9 present the kinetic curves of the mole number of absorbed methane  $n_h$  vs time  $t$  at the initial stage of methane hydrate growth for the studied water–methanol solutions. The calculation of  $n_h$  was carried out according to the procedure described in the supported paper (see equation 3 and last paragraph of Section 2 in ref. [3]). Figs. 10–18 show the averaged methane uptake curves that illustrate the kinetics of methane hydrate crystallization during the whole ramp cooling stage at 1 K/h for each aqueous methanol solution.

**Table 1**

Experimental data on methane hydrate onset temperatures  $T_o$ , pressures  $P_o$ , and subcoolings  $\Delta T_o$  for pure water and aqueous methanol solutions (rocking cell experiments, cooling rate of 1 K/h, initial methane pressure of 8.1 MPa at 295 K); the mean and standard deviation of the indicated values for each sample are shown in bold); the exact composition of each of the aqueous solutions can be found in the original research article (see Table 2 in ref. [3]).

#	Sample	$T_o$ , K	$P_o$ , MPa	$\Delta T_o$ , K
1	H <sub>2</sub> O (0% MeOH)	282.15	7.51	1.41
		281.35	7.46	2.15
		280.55	7.51	3.01
		281.95	7.56	1.67
		280.85	7.5	2.70
		281.75	7.52	1.83
		280.75	7.47	2.77
		280.15	7.41	3.29
		280.35	7.49	3.19
		281.15	7.54	2.45
		280.15	7.46	3.35
		281.85	7.53	1.74
		281.05	7.46	2.45
		280.05	7.41	3.39
		280.65	7.51	2.91
		280.45	7.51	3.11
		279.65	7.43	3.82
281.15	7.49	2.39		
		<b>280.89 ± 0.72</b>	<b>7.49 ± 0.04</b>	<b>2.65 ± 0.68</b>
2	1% MeOH	281.55	7.51	1.64
		281.15	7.52	2.06
		280.85	7.49	2.32
		281.15	7.52	2.06
		280.45	7.47	2.70
		281.15	7.52	2.06
		280.15	7.46	2.98
		281.55	7.52	1.66
		281.05	7.48	2.11
		281.15	7.51	2.04
		<b>281.02 ± 0.44</b>	<b>7.50 ± 0.02</b>	<b>2.16 ± 0.42</b>
3	2.5% MeOH	281.05	7.50	1.54
		280.85	7.51	1.75
		281.25	7.51	1.35
		281.05	7.51	1.55
		280.25	7.50	2.34
		280.65	7.49	1.93
		280.65	7.49	1.93
		<b>280.85 ± 0.36</b>	<b>7.50 ± 0.01</b>	<b>1.75 ± 0.35</b>
4	5% MeOH	280.25	7.47	1.13
		280.25	7.48	1.14
		280.15	7.46	1.22
		279.75	7.46	1.62
		279.45	7.44	1.89
		280.15	7.47	1.23
		280.05	7.45	1.30
		279.55	7.44	1.79
		279.55	7.44	1.79
		<b>279.95 ± 0.32</b>	<b>7.46 ± 0.01</b>	<b>1.42 ± 0.31</b>
5	10% MeOH	277.95	7.34	0.97
		277.75	7.32	1.14
		278.05	7.32	0.84
		277.65	7.35	1.28
		278.25	7.39	0.73
		277.75	7.35	1.18
		277.75	7.35	1.18
		277.85	7.37	1.11
		278.05	7.35	0.88
		277.85	7.35	0.88
		<b>277.89 ± 0.19</b>	<b>7.35 ± 0.02</b>	<b>1.04 ± 0.19</b>

(continued on next page)

Table 1 (continued)

#	Sample	$T_0$ , K	$P_0$ , MPa	$\Delta T_0$ , K		
6	20% MeOH	272.15	7.23	1.23		
		272.95	7.26	0.47		
		272.95	7.27	0.48		
		272.95	7.28	0.49		
		273.15	7.30	0.32		
		273.25	7.28	0.19		
		<b>272.90 ± 0.39</b>	<b>7.27 ± 0.02</b>	<b>0.53 ± 0.36</b>		
7	30% MeOH	264.95	6.90	1.48		
		265.75	6.93	0.72		
		265.35	6.94	1.13		
		265.25	6.93	1.22		
		265.55	6.92	0.91		
		265.55	6.95	0.95		
		265.75	6.95	0.75		
		266.05	6.97	0.47		
		265.95	6.95	0.55		
		265.75	6.94	0.73		
		266.05	6.96	0.46		
		265.85	6.94	0.63		
		265.65	6.91	0.79		
		266.15	6.97	0.37		
		265.75	6.94	0.73		
		<b>265.69 ± 0.32</b>	<b>6.94 ± 0.02</b>	<b>0.79 ± 0.30</b>		
8	40% MeOH	258.05	6.56	0.77		
		258.25	6.58	0.60		
		256.45	6.54	2.34		
		258.96	6.66	0.00 <sup>a</sup>		
		257.85	6.62	1.06		
		256.75	6.58	2.10		
		258.75	6.65	0.20		
		258.35	6.65	0.60		
		255.85	6.52	2.91		
		259.19	6.69	-0.22 <sup>a</sup>		
		258.95	6.64	-0.02 <sup>a</sup>		
		256.85	6.55	1.96		
				<b>257.85 ± 1.11</b>	<b>6.60 ± 0.06</b>	<b>1.02 ± 1.05</b>
		9	50% MeOH	248.15 <sup>b</sup>	6.23 <sup>b</sup>	2.34 <sup>b</sup>
250.85	6.28			-0.29 <sup>a</sup>		
248.15 <sup>b</sup>	6.25 <sup>b</sup>			2.37 <sup>b</sup>		
248.15 <sup>b</sup>	6.23 <sup>b</sup>			2.34 <sup>b</sup>		
248.15 <sup>b</sup>	6.22 <sup>b</sup>			2.32 <sup>b</sup>		
no hydrate <sup>c</sup>	no hydrate <sup>c</sup>			no hydrate <sup>c</sup>		
249.35	6.28			1.21		
248.15 <sup>b</sup>	6.21 <sup>b</sup>			2.30 <sup>b</sup>		
248.15 <sup>b</sup>	6.22 <sup>b</sup>			2.32 <sup>b</sup>		
248.75	6.26			1.78		
248.35	6.25			2.17		
		no hydrate <sup>c</sup>	no hydrate <sup>c</sup>			
		<b>&lt; 248.54 ± 0.81</b>	<b>&lt; 6.24 ± 0.02</b>	<b>&gt; 1.96 ± 0.79</b>		

<sup>a</sup> The slightly negative subcooling value (close to 0) is a result of the accumulated total error in pressure, temperature, and MeOH concentration when 1) measuring the V-L<sub>w</sub>-H equilibrium for aqueous methanol solution; 2) approximating the obtained data with an analytical function; and 3) performing a separate rocking cell experiment with the calculation of  $\Delta T_0$  based on  $T_0$  and  $P_0$  data and the results of steps 1) and 2).

<sup>b</sup> The formation of methane hydrate occurred in the isothermal section at 248.15 K (instead of 1 K/h cooling) due to the cooling limit of the thermostat.

<sup>c</sup> No hydrate was formed even at the end of the isothermal section (275 min at 248.15 K and 6.24 MPa).

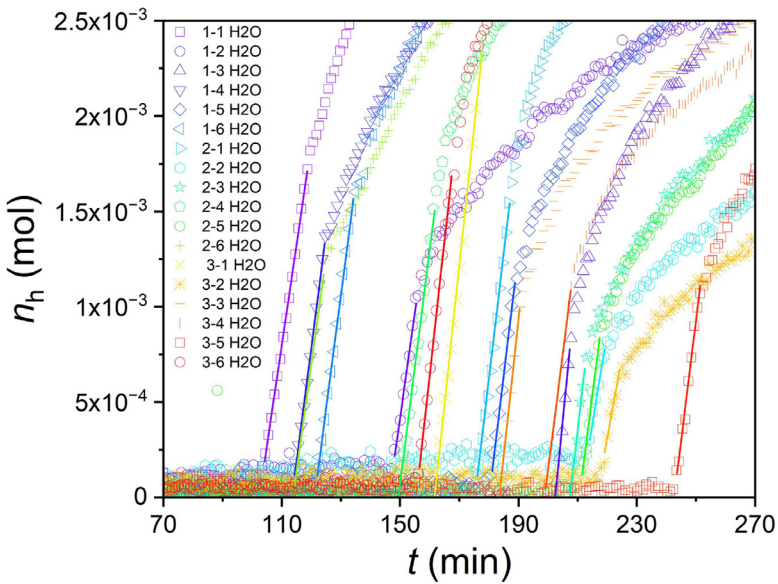


**Fig. 1.** Moles of methane bound to hydrate as a function of time in the initial growth stage during cooling at 1 K/h (pure H<sub>2</sub>O); color symbols are experimental values for all runs, solid lines are linear fits for the initial hydrate growth stage; the first and second digits in the legend reflect the number of cooling-heating cycles and the number of cells;  $t = 0$  corresponds to the intersection of the  $P$ - $T$  trajectory and the V-L<sub>w</sub>-H equilibrium curve for CH<sub>4</sub>-H<sub>2</sub>O (data from [20]).

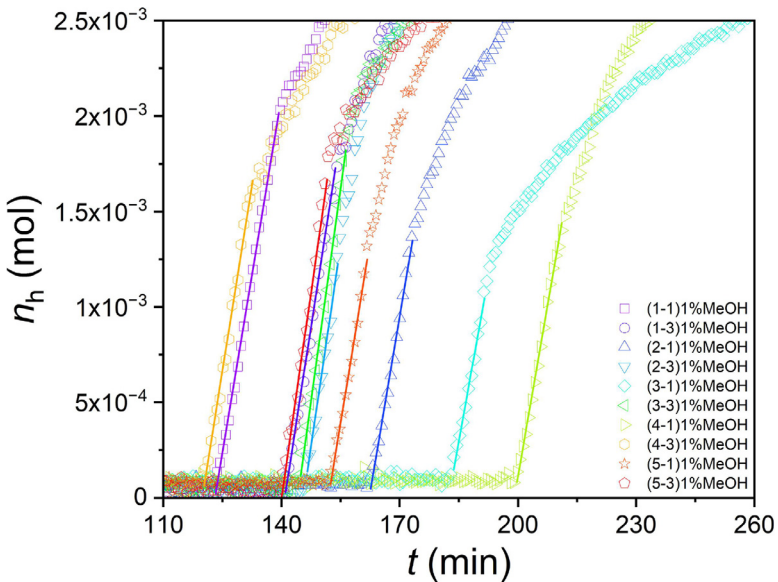


**Fig. 2.** Moles of methane bound to hydrate as a function of time in the initial growth stage during cooling at 1 K/h (1 mass% MeOH); color symbols are experimental values for all runs, solid lines are linear fits for the initial hydrate growth stage; the first and second digits in the legend reflect the number of cooling-heating cycles and the number of cells;  $t = 0$  corresponds to the intersection of the  $P$ - $T$  trajectory and the V-L<sub>w</sub>-H equilibrium curve for CH<sub>4</sub>-MeOH-H<sub>2</sub>O (data from [1,2]).

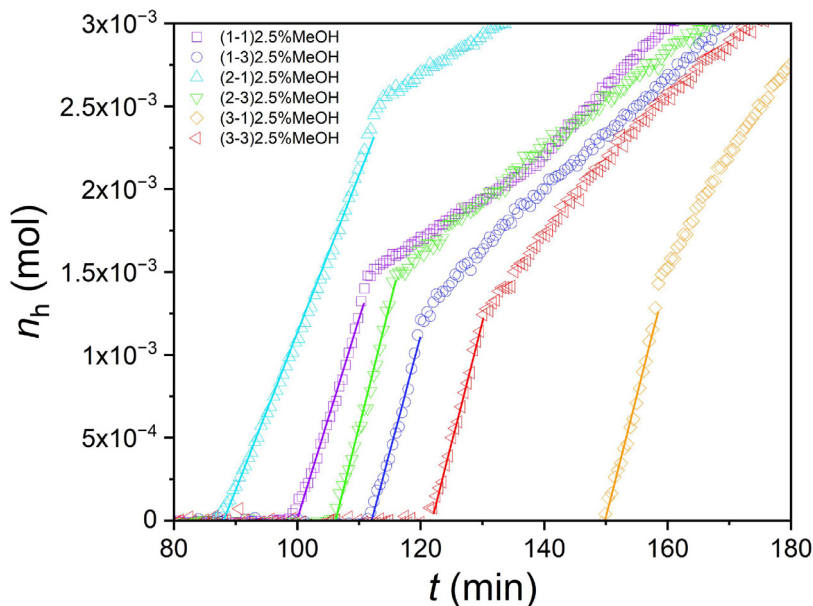


**Fig. 3.** Moles of methane bound to hydrate as a function of time in the initial growth stage during cooling at 1 K/h (2.5 mass% MeOH); color symbols are experimental values for all runs, solid lines are linear fits for the initial hydrate growth stage; the first and second digits in the legend reflect the number of cooling-heating cycles and the number of cells;  $t = 0$  corresponds to the intersection of the  $P$ - $T$  trajectory and the  $V$ - $L_w$ - $H$  equilibrium curve for  $\text{CH}_4$ - $\text{MeOH}$ - $\text{H}_2\text{O}$  (data from [1,2]).

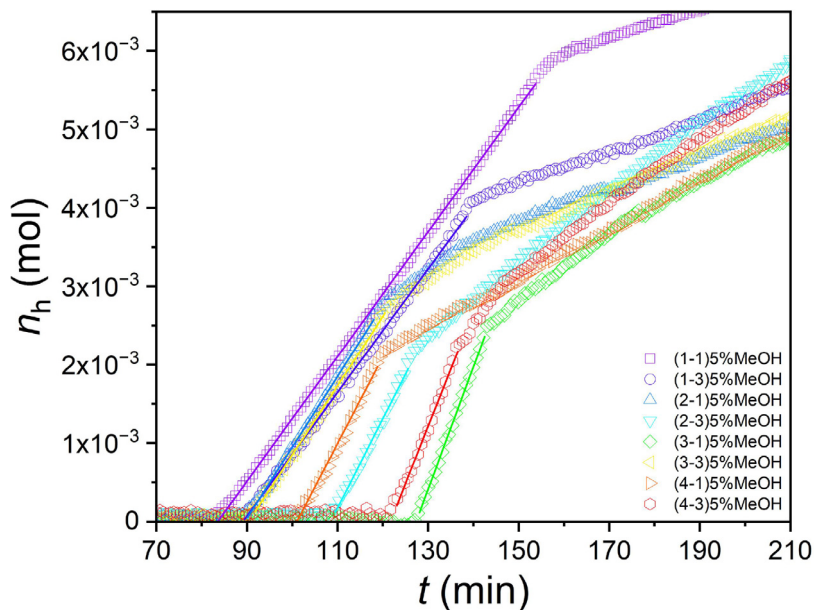


**Fig. 4.** Moles of methane bound to hydrate as a function of time in the initial growth stage during cooling at 1 K/h (5 mass% MeOH); color symbols are experimental values for all runs, solid lines are linear fits for the initial hydrate growth stage; the first and second digits in the legend reflect the number of cooling-heating cycles and the number of cells;  $t = 0$  corresponds to the intersection of the  $P$ - $T$  trajectory and the  $V$ - $L_w$ - $H$  equilibrium curve for  $\text{CH}_4$ - $\text{MeOH}$ - $\text{H}_2\text{O}$  (data from [1,2]).

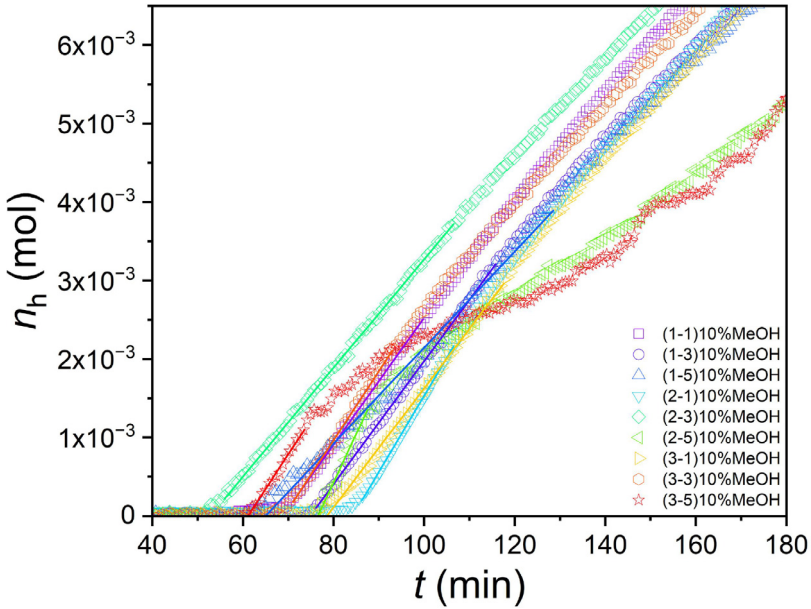


**Fig. 5.** Moles of methane bound to hydrate as a function of time in the initial growth stage during cooling at 1 K/h (10 mass% MeOH); color symbols are experimental values for all runs, solid lines are linear fits for the initial hydrate growth stage; the first and second digits in the legend reflect the number of cooling-heating cycles and the number of cells;  $t = 0$  corresponds to the intersection of the  $P$ - $T$  trajectory and the  $V$ - $L_w$ - $H$  equilibrium curve for  $\text{CH}_4$ -MeOH- $\text{H}_2\text{O}$  (data from [1,2]).

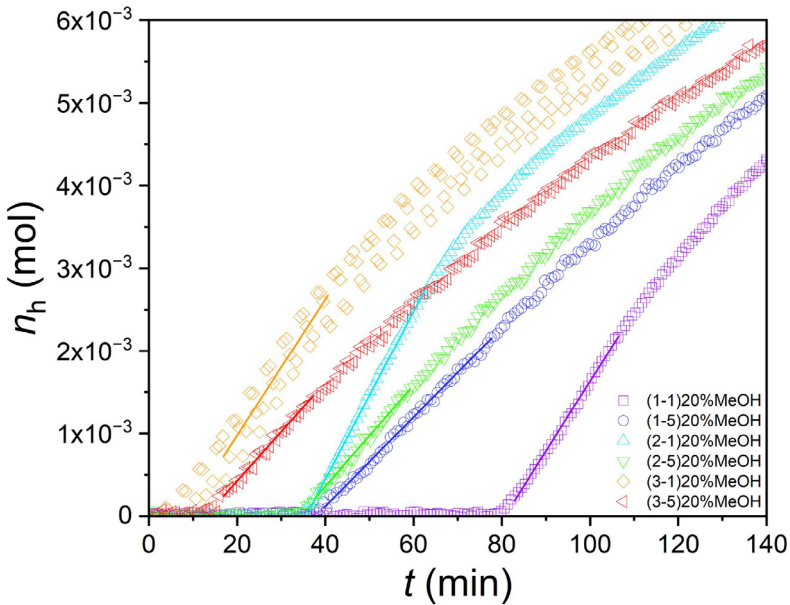


**Fig. 6.** Moles of methane bound to hydrate as a function of time in the initial growth stage during cooling at 1 K/h (20 mass% MeOH); color symbols are experimental values for all runs, solid lines are linear fits for the initial hydrate growth stage; the first and second digits in the legend reflect the number of cooling-heating cycles and the number of cells;  $t = 0$  corresponds to the intersection of the  $P$ - $T$  trajectory and the  $V$ - $L_w$ - $H$  equilibrium curve for  $\text{CH}_4$ -MeOH- $\text{H}_2\text{O}$  (data from [1,2]).

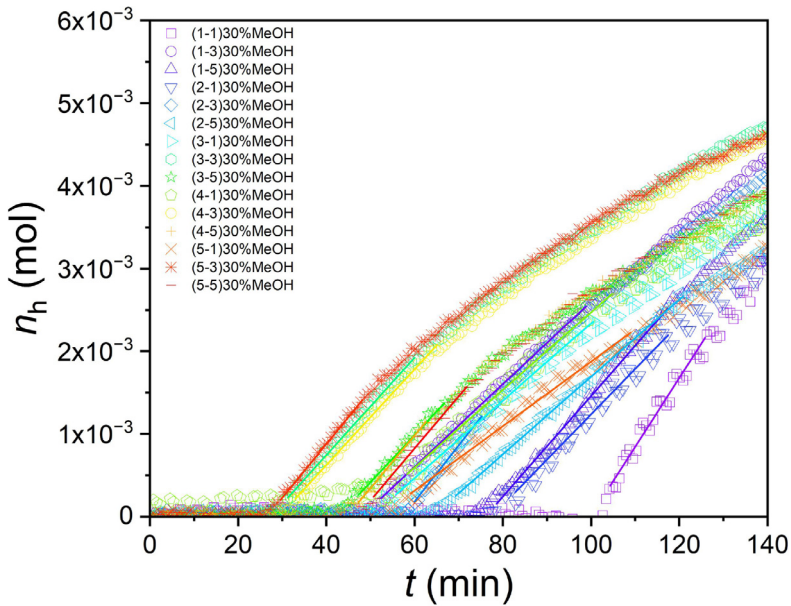


**Fig. 7.** Moles of methane bound to hydrate as a function of time in the initial growth stage during cooling at 1 K/h (30 mass% MeOH); color symbols are experimental values for all runs, solid lines are linear fits for the initial hydrate growth stage; the first and second digits in the legend reflect the number of cooling-heating cycles and the number of cells;  $t = 0$  corresponds to the intersection of the  $P$ - $T$  trajectory and the  $V$ - $L_w$ - $H$  equilibrium curve for  $\text{CH}_4$ -MeOH- $\text{H}_2\text{O}$  (data from [1,2]).

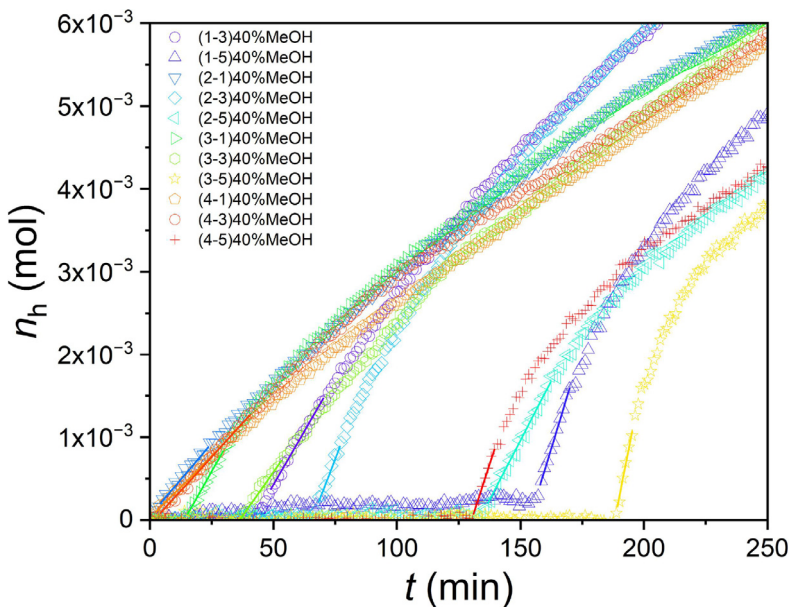


**Fig. 8.** Moles of methane bound to hydrate as a function of time in the initial growth stage during cooling at 1 K/h (40 mass% MeOH); color symbols are experimental values for all runs, solid lines are linear fits for the initial hydrate growth stage; the first and second digits in the legend reflect the number of cooling-heating cycles and the number of cells;  $t = 0$  corresponds to the intersection of the  $P$ - $T$  trajectory and the  $V$ - $L_w$ - $H$  equilibrium curve for  $\text{CH}_4$ -MeOH- $\text{H}_2\text{O}$  (data from [1,2]).

**Table 2**

Parameters of gamma cumulative distribution functions describing dependency  $F(\Delta T_0)$  for aqueous methanol solution. Adjusted parameters  $F_0$  and  $A_1$  of gamma cumulative distribution function are fixed ( $F_0 = 0, A_1 = 1$ ) as the cumulative probability of hydrate nucleation varies from 0 to 1.

#	Methanol fraction, mass%	Shape parameter $a$		Scale parameter $b$		Adjusted $R^2$
		Value	Standard Error	Value	Standard Error	
1	0	11.6492	1.1136	0.2401	0.0233	0.9680
2	1	17.3766	5.2295	0.1278	0.0397	0.8544
3	2.5	12.9517	4.0722	0.1422	0.0466	0.8840
4	5	10.0273	2.4270	0.1485	0.0377	0.8856
5	10	18.9019	4.0140	0.0578	0.0124	0.9160
6	20	1.4262	0.6057	0.4763	0.2692	0.7769
7	30	5.7444	0.6683	0.1442	0.0180	0.9597
8	40	0.7353	0.1170	2.2614	0.5250	0.9150

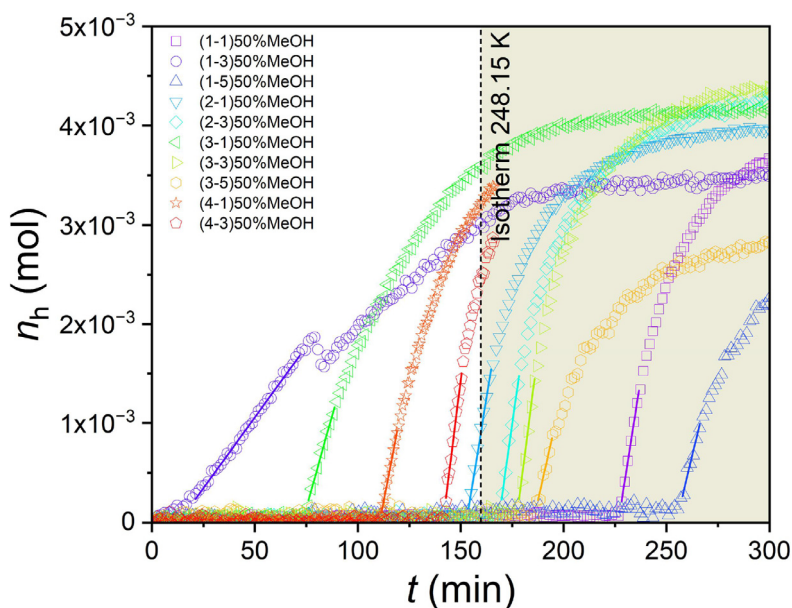


**Fig. 9.** Moles of methane bound to hydrate as a function of time for sample 50 mass% MeOH in the initial growth stage during cooling (1 K/h ramp cooling until 159.7 min to 248.15 K, then constant temperature of 248.15 K because of the cooling limit of the thermostat); color symbols are experimental values for all runs, solid lines are linear fits for the initial hydrate growth stage; the first and second digits in the legend reflect the number of cooling-heating cycles and the number of cells;  $t = 0$  corresponds to the intersection of the  $P$ - $T$  trajectory and the  $V$ - $L_w$ - $H$  equilibrium curve for  $\text{CH}_4$ - $\text{MeOH}$ - $\text{H}_2\text{O}$  (data from [1,2]).

#### 4. Experimental Design, Materials and Methods

The chemicals used in the experiment were methanol (Himed, Russian Federation) with a main component content of not less than 99.7 mass%, deionized water with a resistivity of 18.2 Mohm·cm (at 298 K), and pressurized methane gas with a purity of not less than 99.99 vol% (Moscow Gas Processing Plant, Russian Federation). Aqueous solutions of methanol were prepared gravimetrically. For this purpose, methanol and deionized water were added sequentially to a 100 mL glass conical flask. Each solution was prepared in a quantity of 70 g, and the mass of each component was controlled to 0.001 g using a PA413C balance (Ohaus Pioneer, USA). De-

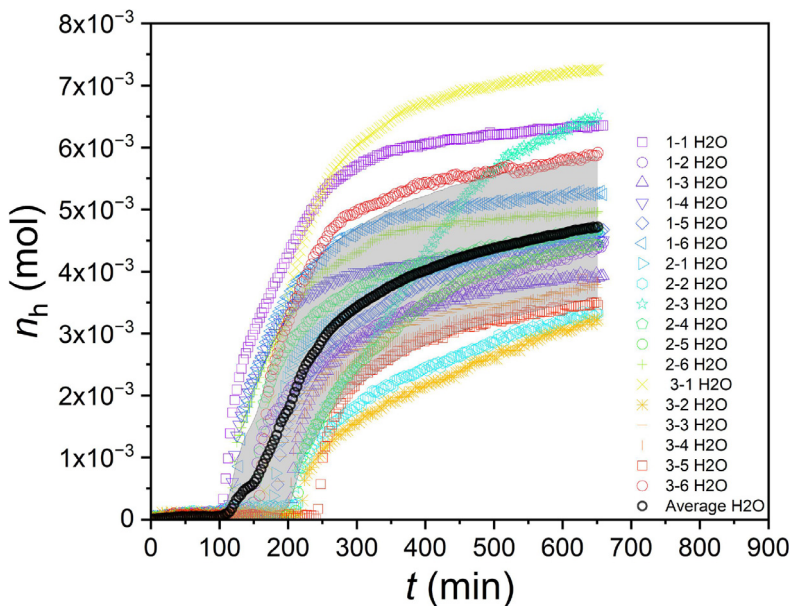


**Fig. 10.** Kinetic curves of methane amount in hydrate versus time during cooling at 1 K/h (pure H<sub>2</sub>O); color symbols are experimental values for all runs, black circles show the mean curve, gray fill corresponds to the standard deviation of the mean; the first and second digits in the legend reflect the number of cooling-heating cycles and the number of cells;  $t = 0$  corresponds to the intersection of the  $P$ - $T$  trajectory and the V-L<sub>w</sub>-H equilibrium curve for CH<sub>4</sub>-H<sub>2</sub>O (data from [20]).

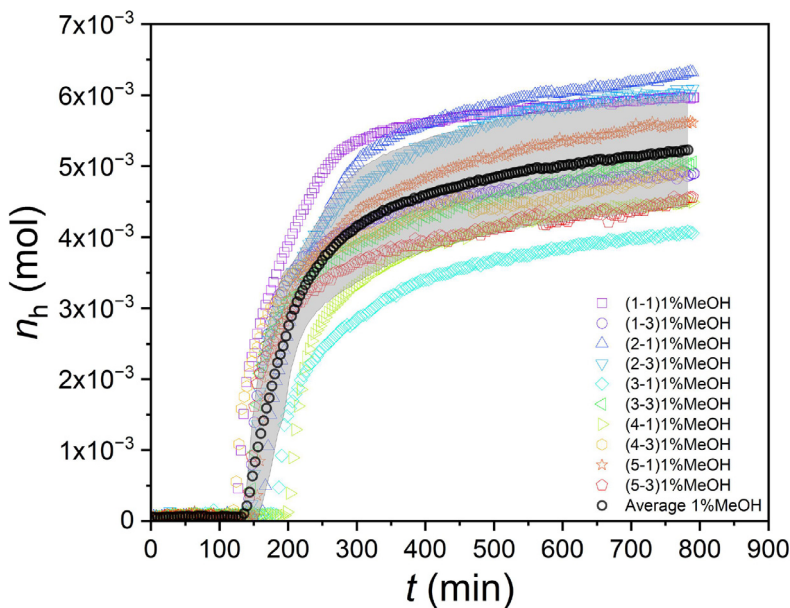


**Fig. 11.** Kinetic curves of methane amount in hydrate versus time during cooling at 1 K/h (1 mass% MeOH); color symbols are experimental values for all runs, black circles show the mean curve, gray fill corresponds to the standard deviation of the mean; the first and second digits in the legend reflect the number of cooling-heating cycles and the number of cells;  $t = 0$  corresponds to the intersection of the  $P$ - $T$  trajectory and the V-L<sub>w</sub>-H equilibrium curve for CH<sub>4</sub>-MeOH-H<sub>2</sub>O (data from [1,2]).

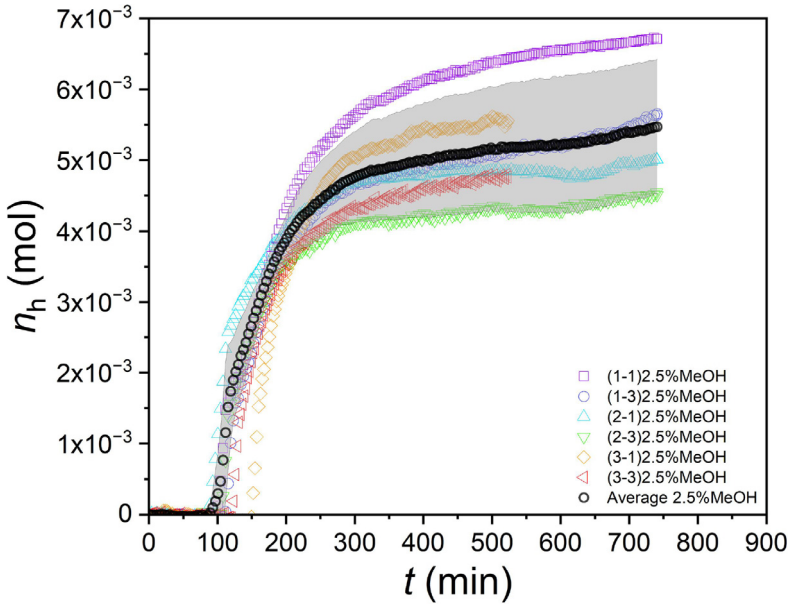


**Fig. 12.** Kinetic curves of methane amount in hydrate versus time during cooling at 1 K/h (2.5 mass% MeOH); color symbols are experimental values for all runs, black circles show the mean curve, gray fill corresponds to the standard deviation of the mean; the first and second digits in the legend reflect the number of cooling-heating cycles and the number of cells;  $t = 0$  corresponds to the intersection of the  $P$ - $T$  trajectory and the  $V$ - $L_w$ - $H$  equilibrium curve for  $\text{CH}_4$ -MeOH- $\text{H}_2\text{O}$  (data from [1,2]).

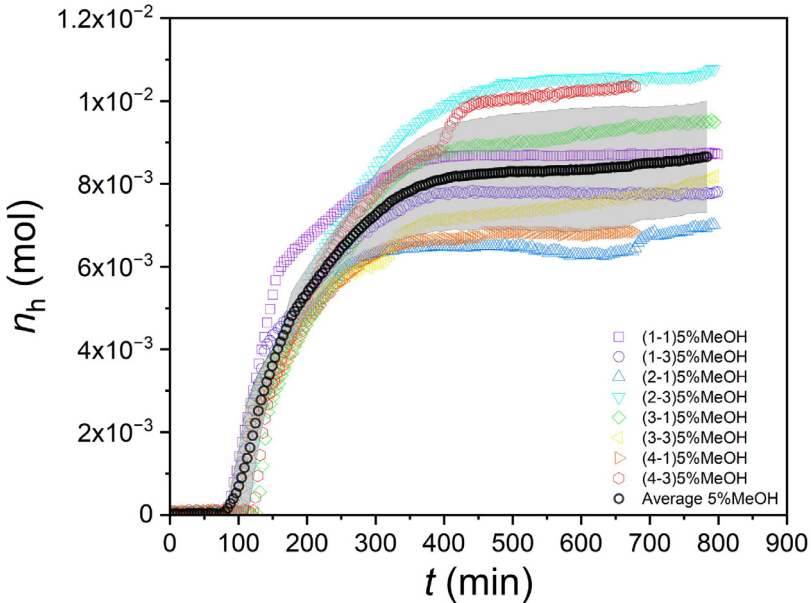


**Fig. 13.** Kinetic curves of methane amount in hydrate versus time during cooling at 1 K/h (5 mass% MeOH); color symbols are experimental values for all runs, black circles show the mean curve, gray fill corresponds to the standard deviation of the mean; the first and second digits in the legend reflect the number of cooling-heating cycles and the number of cells;  $t = 0$  corresponds to the intersection of the  $P$ - $T$  trajectory and the  $V$ - $L_w$ - $H$  equilibrium curve for  $\text{CH}_4$ -MeOH- $\text{H}_2\text{O}$  (data from [1,2]).

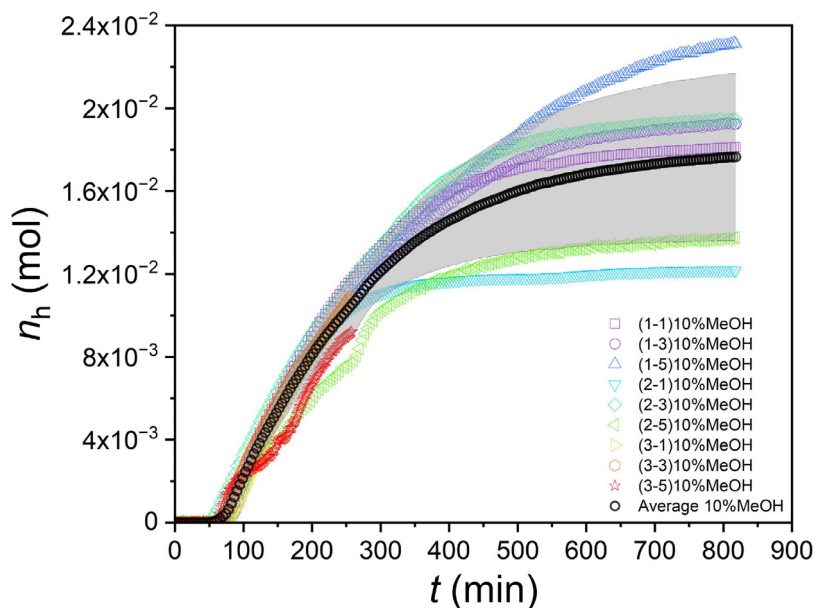


**Fig. 14.** Kinetic curves of methane amount in hydrate versus time during cooling at 1 K/h (10 mass% MeOH); color symbols are experimental values for all runs, black circles show the mean curve, gray fill corresponds to the standard deviation of the mean; the first and second digits in the legend reflect the number of cooling-heating cycles and the number of cells;  $t = 0$  corresponds to the intersection of the  $P$ - $T$  trajectory and the  $V$ - $L_w$ - $H$  equilibrium curve for  $\text{CH}_4$ -MeOH- $\text{H}_2\text{O}$  (data from [1,2]).

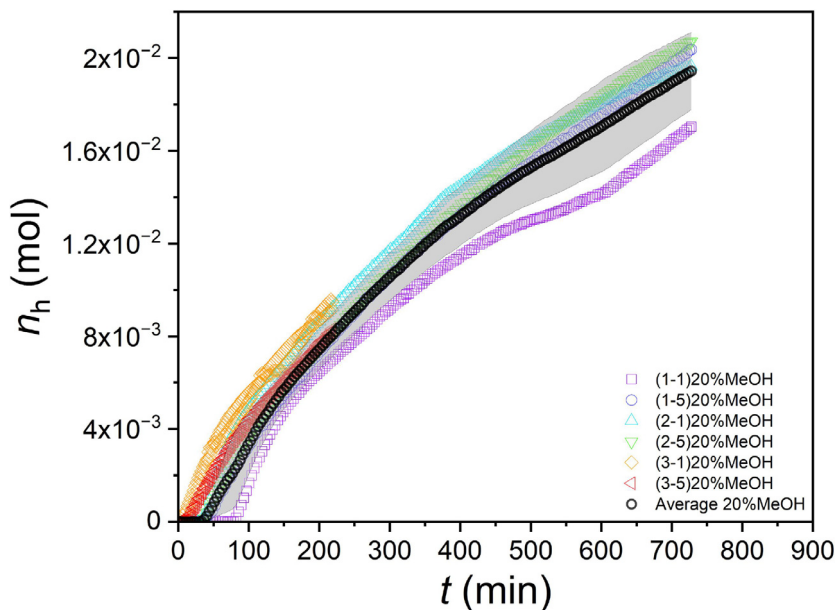


**Fig. 15.** Kinetic curves of methane amount in hydrate versus time during cooling at 1 K/h (20 mass% MeOH); color symbols are experimental values for all runs, black circles show the mean curve, gray fill corresponds to the standard deviation of the mean; the first and second digits in the legend reflect the number of cooling-heating cycles and the number of cells;  $t = 0$  corresponds to the intersection of the  $P$ - $T$  trajectory and the  $V$ - $L_w$ - $H$  equilibrium curve for  $\text{CH}_4$ -MeOH- $\text{H}_2\text{O}$  (data from [1,2]).

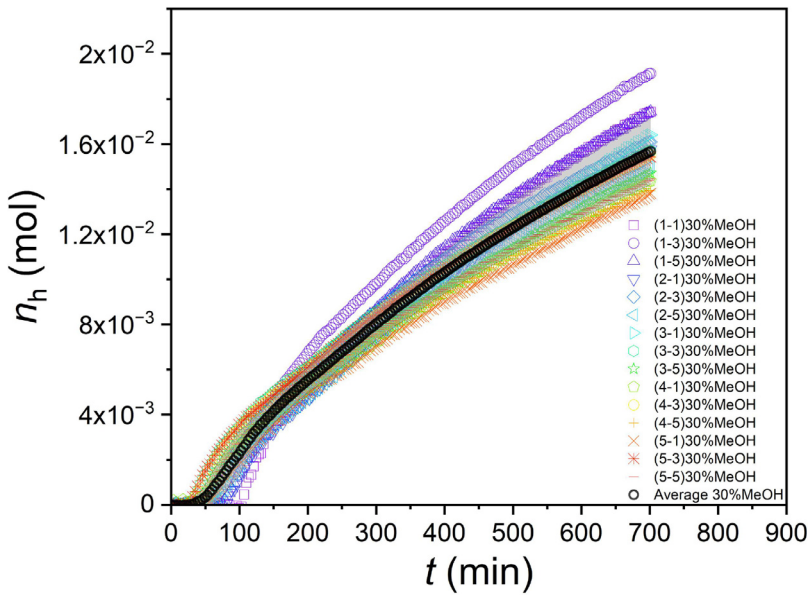


**Fig. 16.** Kinetic curves of methane amount in hydrate versus time during cooling at 1 K/h (30 mass% MeOH); color symbols are experimental values for all runs, black circles show the mean curve, gray fill corresponds to the standard deviation of the mean; the first and second digits in the legend reflect the number of cooling-heating cycles and the number of cells;  $t = 0$  corresponds to the intersection of the  $P$ - $T$  trajectory and the  $V$ - $L_w$ - $H$  equilibrium curve for  $\text{CH}_4$ - $\text{MeOH}$ - $\text{H}_2\text{O}$  (data from [1,2]).

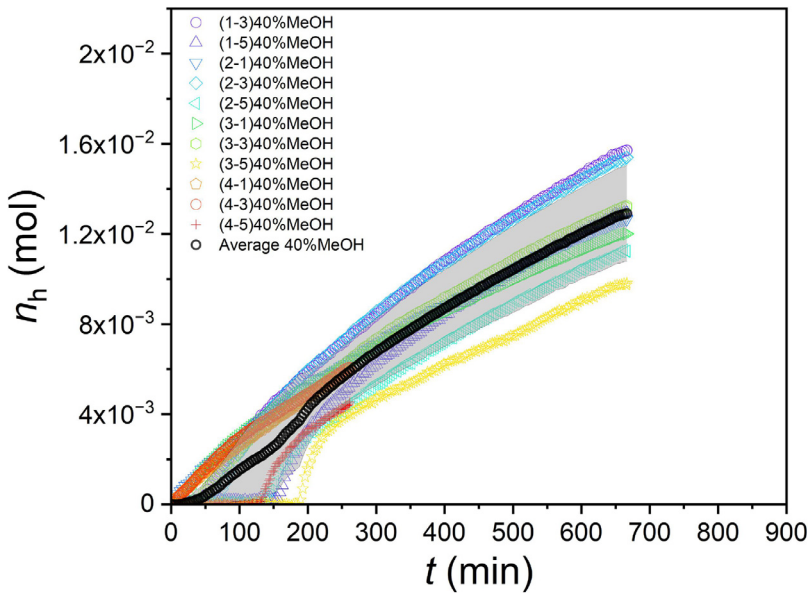


**Fig. 17.** Kinetic curves of methane amount in hydrate versus time during cooling at 1 K/h (40 mass% MeOH); color symbols are experimental values for all runs, black circles show the mean curve, gray fill corresponds to the standard deviation of the mean; the first and second digits in the legend reflect the number of cooling-heating cycles and the number of cells;  $t = 0$  corresponds to the intersection of the  $P$ - $T$  trajectory and the  $V$ - $L_w$ - $H$  equilibrium curve for  $\text{CH}_4$ - $\text{MeOH}$ - $\text{H}_2\text{O}$  (data from [1,2]).

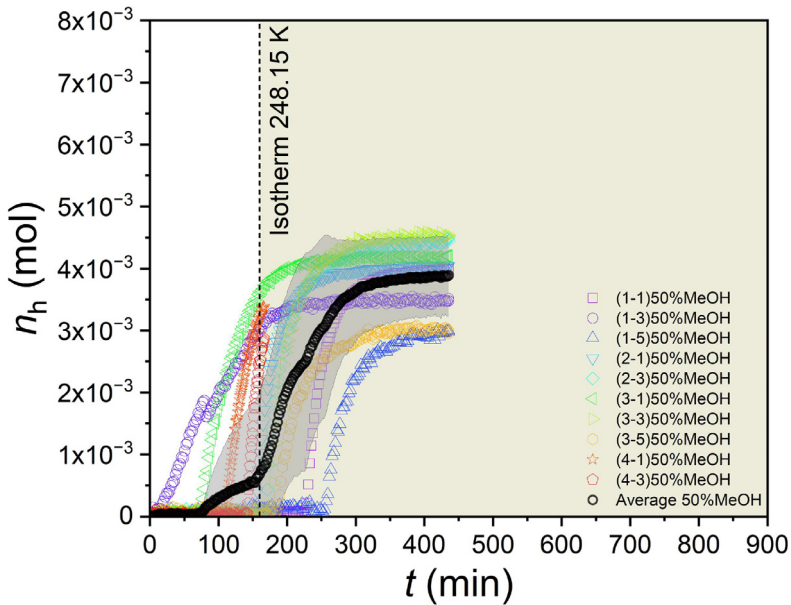


**Fig. 18.** Kinetic curves of methane amount in hydrate versus time for sample 50 mass% MeOH during cooling (1 K/h ramp cooling until 159.7 min to 248.15 K, then constant temperature of 248.15 K because of the cooling limit of the thermostat); color symbols are experimental values for all runs, black circles show the mean curve, gray fill corresponds to the standard deviation of the mean; the first and second digits in the legend reflect the number of cooling-heating cycles and the number of cells;  $t = 0$  corresponds to the intersection of the  $P$ - $T$  trajectory and the  $V$ - $L_w$ - $H$  equilibrium curve for  $\text{CH}_4$ -MeOH- $\text{H}_2\text{O}$  (data from [1,2]).

tailed information on the composition of the aqueous methanol solutions is given in the original research paper (see Table 2 in ref [3]).

Experiments were conducted to study the kinetics of nucleation and growth of methane hydrate using the Sapphire Rocking Cells RCS6 (PSL Systemtechnik, Germany), which is described in the previous paper [1]. In each cell of the setup, we added 10 mL of the investigated aqueous methanol solution of a given concentration and a stainless-steel ball of 10 mm diameter, which serves for more effective mixing of the fluids in the cell during rocking and minimizes the induction time of methane hydrate formation. The cells were flushed with methane gas as follows. Methane was injected into the free volume at a pressure of 1 MPa and a temperature of 295 K. The gas was then vented by reducing the pressure to an atmospheric level of 100 kPa. This procedure was repeated three times. Next, methane was injected up to a pressure of 8.1 MPa at 295 K, and the air concentration in the free volume of the cells was reduced to a trace level (about 12 ppm). After injecting methane, each apparatus cell was sealed by closing the ball valve. The cells were tilted at an angle of  $\pm 45^\circ$  with a frequency of  $10 \text{ min}^{-1}$  during the experiment. The coolant temperature in the bath, a mixture of water and ethylene glycol 1:1 by mass, was varied according to the following program. In the initial step, the temperature in the bath was lowered to such a value that the  $P$ - $T$  conditions in the cells were outside the hydrate stability zone for the studied methanol solution but close to the curve of the three-phase vapor-aqueous solution-gas hydrate equilibrium (based on experimental data [1,2]), taking into account the alcohol content in the solution. The system was held at the first step for 1 hour. During the second step, the bath temperature was decreased at a constant rate of 1 K/h by 11–12 K. The methane hydrate formation occurred during the second step after crossing the experimental  $P$ - $T$  trajectory and the three-phase gas-water solution-gas hydrate equilibrium line. The start of methane hydrate growth was detected by the appearance of a kink in the  $P$ - $T$  trajectory caused by gas uptake following the completion of the nucleation stage (see Fig. 1 from

the supported article [3]). After the end of the second part of the temperature program, the cells were heated to 306 K and held for 3 hours, which resulted in the complete decomposition of the formed methane hydrate and the return of the system to the initial two-phase state of gaseous methane–aqueous methanol solution. The temperature program was repeated several times for each sample to verify the reproducibility of the results and to obtain a statistically significant dataset (at least 6 measurements for each methanol concentration). The third step of the temperature program (holding for 3 h at 306 K) eliminated the memory effect (hydrate formation at higher temperature and lower subcooling) in subsequent cooling-heating cycles.

## Limitations

Not applicable.

## Ethics Statement

The studies described in the manuscript adhered to Ethics in publishing standards (<https://www.elsevier.com/journals/data-in-brief/2352-3409/guide-for-authors>) and did not involve human or animal subjects.

## Data Availability

Raw data from the investigation of methane hydrate nucleation and growth kinetics in the methane–water and methane–methanol–water systems (Original data) (Mendeley Data).

## CRediT Author Statement

**Anton P. Semenov:** Data curation, Visualization, Writing – original draft, Validation, Writing – review & editing; **Timur B. Tulegenov:** Investigation; **Rais I. Mendgaziev:** Investigation; **Andrey S. Stoporev:** Visualization, Writing – original draft, Writing – review & editing; **Vladimir A. Istomin:** Supervision; **Daria V. Sergeeva:** Investigation; **Daniil A. Lednev:** Investigation; **Vladimir A. Vinokurov:** Resources, Project administration, Funding acquisition.

## Declaration of Competing Interests

The authors declare that they have no known competing financial interests or personal relationships that could have appeared to influence the work reported in this paper.

## References

- [1] A.P. Semenov, Y. Gong, V.I. Medvedev, A.S. Stoporev, V.A. Istomin, V.A. Vinokurov, T. Li, New insights into methane hydrate inhibition with blends of vinyl lactam polymer and methanol, monoethylene glycol, or diethylene glycol as hybrid inhibitors, *Chem. Eng. Sci.* 268 (2023) 118387, doi:10.1016/j.ces.2022.118387.
- [2] A.P. Semenov, Y. Gong, V.I. Medvedev, A.S. Stoporev, V.A. Istomin, V.A. Vinokurov, T. Li, Dataset for the new insights into methane hydrate inhibition with blends of vinyl lactam polymer and methanol, monoethylene glycol, or diethylene glycol as hybrid inhibitors, *Data Br* 46 (2023) 108892, doi:10.1016/j.dib.2023.108892.
- [3] A.P. Semenov, T.B. Tulegenov, R.I. Mendgaziev, A.S. Stoporev, V.A. Istomin, D.V. Sergeeva, D.A. Lednev, V.A. Vinokurov, Dual nature of methanol as a thermodynamic inhibitor and kinetic promoter of methane hydrate formation in a wide concentration range, *J. Mol. Liq.* 403 (2024) 124780, doi:10.1016/j.molliq.2024.124780.
- [4] H.J. Ng, D.B. Robinson, Hydrate formation in systems containing methane, ethane, propane, carbon dioxide or hydrogen sulfide in the presence of methanol, *Fluid Phase Equilib.* 21 (1985) 145–155, doi:10.1016/0378-3812(85)90065-2.

- [5] D.B. Robinson, H.J. Ng, Hydrate formation and inhibition in gas or gas condensate streams, *J. Can. Pet. Technol.* 25 (1986) 26–30, doi:[10.2118/86-04-01](https://doi.org/10.2118/86-04-01).
- [6] H. Haghighi, A. Chapoy, R. Burgess, S. Mazloum, B. Tohidi, Phase equilibria for petroleum reservoir fluids containing water and aqueous methanol solutions: experimental measurements and modelling using the CPA equation of state, *Fluid Phase Equilib.* 278 (2009) 109–116, doi:[10.1016/j.fluid.2009.01.009](https://doi.org/10.1016/j.fluid.2009.01.009).
- [7] A.H. Mohammadi, D. Richon, Phase equilibria of methane hydrates in the presence of methanol and/or ethylene glycol aqueous solutions, *Ind. Eng. Chem. Res.* 49 (2010) 925–928, doi:[10.1021/ie901357m](https://doi.org/10.1021/ie901357m).
- [8] A.P. Semenov, R.I. Mendgaziev, V.A. Istomin, D.V. Sergeeva, V.A. Vinokurov, Y. Gong, T. Li, A.S. Stoporev, Searching for synergy between alcohol and salt to produce more potent and environmentally benign gas hydrate inhibitors, *Chem. Eng. Sci.* 283 (2024) 119361, doi:[10.1016/j.ces.2023.119361](https://doi.org/10.1016/j.ces.2023.119361).
- [9] A.P. Semenov, R.I. Mendgaziev, V.A. Istomin, D.V. Sergeeva, V.A. Vinokurov, Y. Gong, T. Li, A.S. Stoporev, Data on searching for synergy between alcohol and salt to produce more potent and environmentally benign gas hydrate inhibitors, *Data Br.* 53 (2024) 110138, doi:[10.1016/j.dib.2024.110138](https://doi.org/10.1016/j.dib.2024.110138).
- [10] A.A. Krasnov, V.B. Klimentok, Study of kinetics of clathration processes by isochron method [in Russian], *Neftekhimiya* 13 (1973) 592–595.
- [11] S.V. Amel'kin, V.P. Mel'nikov, A.N. Nesterov, Kinetics of growth of gas hydrates in dilute solutions of nonelectrolyte inhibitors, *Colloid J.* 62 (2000) 401–406.
- [12] H.K. Abay, T.M. Svartaas, Effect of ultralow concentration of methanol on methane hydrate formation, *Energy and Fuels* 24 (2010) 752–757, doi:[10.1021/ef9009422](https://doi.org/10.1021/ef9009422).
- [13] G. McLaurin, K. Shin, S. Alavi, J.A. Ripmeester, Antifreezes act as catalysts for methane hydrate formation from ice, *Angew. Chemie.* 126 (2014) 10597–10601, doi:[10.1002/ange.201403638](https://doi.org/10.1002/ange.201403638).
- [14] J. Amtawong, J. Guo, J.S. Hale, S. Sengupta, E.B. Fleischer, R.W. Martin, K.C. Janda, Propane clathrate hydrate formation accelerated by methanol, *J. Phys. Chem. Lett.* 7 (2016) 2346–2349, doi:[10.1021/acs.jpcclett.6b00982](https://doi.org/10.1021/acs.jpcclett.6b00982).
- [15] Z. Su, S. Alavi, J.A. Ripmeester, G. Wolosh, C.L. Dias, Methane clathrate formation is catalyzed and kinetically inhibited by the same molecule: two facets of methanol, *J. Phys. Chem. B.* 125 (2021) 4162–4168, doi:[10.1021/acs.jpcc.1c01274](https://doi.org/10.1021/acs.jpcc.1c01274).
- [16] M. Lauricella, M.R. Ghaani, P.K. Nandi, S. Meloni, B. Kvamme, N.J. English, Double life of methanol: experimental studies and nonequilibrium molecular-dynamics simulation of methanol effects on methane-hydrate nucleation, *J. Phys. Chem. C.* 126 (2022) 6075–6081, doi:[10.1021/acs.jpcc.2c00329](https://doi.org/10.1021/acs.jpcc.2c00329).
- [17] J.S. Pandey, S. Khan, N. von Solms, Screening of low-dosage methanol as a hydrate promoter, *Energies* 15 (2022) 6814, doi:[10.3390/en15186814](https://doi.org/10.3390/en15186814).
- [18] A.P. Semenov, T.B. Tulegenov, R.I. Mendgaziev, A.S. Stoporev, V.A. Istomin, V.A. Vinokurov, Effect of methanol on the kinetics of nucleation and growth of methane hydrate, *Chem. Technol. Fuels Oils.* 59 (2023) 667–672, doi:[10.1007/s10553-023-01567-9](https://doi.org/10.1007/s10553-023-01567-9).
- [19] J. Zhang, Z. Wang, L. Li, Y. Yan, J. Xu, J. Zhong, New insights into the kinetic effects of CH<sub>3</sub>OH on methane hydrate nucleation, *Energy* 263 (2023) 125824, doi:[10.1016/j.energy.2022.125824](https://doi.org/10.1016/j.energy.2022.125824).
- [20] A.P. Semenov, R.I. Mendgaziev, A.S. Stoporev, Dataset for the experimental study of dimethyl sulfoxide as a thermodynamic inhibitor of methane hydrate formation, *Data Br.* 48 (2023) 109283, doi:[10.1016/j.dib.2023.109283](https://doi.org/10.1016/j.dib.2023.109283).